PLOS ONE

The aerobic respiratory chain of *Pseudomonas aeruginosa* cultured in artificial urine media: Role of NQR and terminal oxidases

Pingdong Liang[1☯], **Xuan Fang**[1☯], **Yuyao Hu**[1☯], **Ming Yuan**[1], **Daniel A. Raba**[1], **Jie Ding**[1], **Dakota C. Bunn**[1], **Krithica Sanjana**[1], **Jun Yang**[1], **Monica Rosas-Lemus**[1], **Claudia C. Häse**[2], **Karina Tuz**[1], **Oscar Juárez**[1] *

1 Department of Biological Sciences, Illinois Institute of Technology, Chicago, IL, United States of America,
2 Carlson College of Veterinary Medicine, Oregon State University, Corvallis, OR, United States of America

☯ These authors contributed equally to this work.
* ojuarez@iit.edu

Abstract

Pseudomonas aeruginosa is a Gram-negative γ-proteobacterium that forms part of the normal human microbiota and it is also an opportunistic pathogen, responsible for 30% of all nosocomial urinary tract infections. *P. aeruginosa* carries a highly branched respiratory chain that allows the colonization of many environments, such as the urinary tract, catheters and other medical devices. *P. aeruginosa* respiratory chain contains three different NADH dehydrogenases (complex I, NQR and NDH-2), whose physiologic roles have not been elucidated, and up to five terminal oxidases: three cytochrome *c* oxidases (COx), a cytochrome *bo*₃ oxidase (CYO) and a cyanide-insensitive cytochrome *bd*-like oxidase (CIO). In this work, we studied the composition of the respiratory chain of *P. aeruginosa* cells cultured in Luria Broth (LB) and modified artificial urine media (mAUM), to understand the metabolic adaptations of this microorganism to the growth in urine. Our results show that the COx oxidases play major roles in mAUM, while *P. aeruginosa* relies on CYO when growing in LB medium. Moreover, our data demonstrate that the proton-pumping NQR complex is the main NADH dehydrogenase in both LB and mAUM. This enzyme is resistant to HQNO, an inhibitory molecule produced by *P. aeruginosa*, and may provide an advantage against the natural antibacterial agents produced by this organism. This work offers a clear picture of the composition of this pathogen's aerobic respiratory chain and the main roles that NQR and terminal oxidases play in urine, which is essential to understand its physiology and could be used to develop new antibiotics against this notorious multidrug-resistant microorganism.

Introduction

Pseudomonas aeruginosa is a Gram-negative, rod shaped γ-proteobacteria that colonizes a large diversity of environments, such as soil, water, and forms part of the normal microbiota of humans, animals and plants [1,2]. *P. aeruginosa* is also an opportunistic human pathogen that commonly infects epidermal burns [3], the lung epithelia of cystic fibrosis patients [4,5] and it

is responsible for one third of all nosocomial urinary tract infections (UTI), which greatly increase the risk of morbidity and mortality in septic shock patients and diabetic patients [6] and are commonly associated with the use of contaminated catheters [7,8]. The World Health Organization ranks *P. aeruginosa* on its critical priority list as the second most important microorganism for the development of new treatments [9]. Thus, it is essential to understand the mechanisms used by this pathogen to survive in the urinary tract and other commonly infected environments.

P. aeruginosa has an enormous repertoire of molecular mechanisms that allow its adaptation to the environment, including a flexible metabolism that plays an essential role in its capability to colonize diverse niches. This bacterium is a facultative anaerobe with a highly branched respiratory chain that uses either oxygen or nitrogen oxides as final electron acceptors [10–12] and that under aerobic conditions uses oxidative phosphorylation, rather than fermentation, to produce ATP [4,11,12]. The genome contains 17 different dehydrogenases [13], 15 of which transfer the electrons from diverse reduced substrates to ubiquinone, and two of them transfer the electrons directly to nitrate reductases or cytochrome *c* [4,13]. The aerobic respiratory chain is also branched at the level of the ubiquinone pool, containing a cytochrome bo_3 oxidase (CYO) and a cyanide-insensitive cytochrome *bd*–like oxidase (CIO), both of which transfer electrons directly from quinol to oxygen (Fig 1A) [12–14]. In addition to the quinol oxidases, the respiratory chain contains cytochrome bc_1 and three cytochrome *c* oxidases (COx): caa_3, cbb_3-1 and cbb_3-2 (Fig 1A) [4].

One of the most striking differences between the respiratory chain of this bacterium and that of human mitochondria is that *P. aeruginosa* possesses three different dehydrogenases that transfer electrons from NADH to the ubiquinone pool: complex I, NQR (formerly Na^+-NQR, see below) and NDH-2 [13,15], while mitochondria only carry complex I. Complex I is a 500 kDa respiratory enzyme composed of 14 subunits and several cofactors: two 2Fe-2S centers, six 4Fe-4S clusters, and a non-covalently bound FMN [16,17]. NQR is composed of six subunits and contains one FAD, two covalently-bound FMNs, one 2Fe-2S center, a riboflavin molecule and possibly a non-heme Fe center [18–22]. NDH-2 is a 46 kDa peripheral protein with a single FAD cofactor [17,23]. The most important physiologic difference between these enzymes is that complex I is a proton pump, while NDH-2 is not involved in ion pumping [17,23]. Although in many cases it has been reported that NQR acts as a sodium pump, we recently described that *P. aeruginosa* NQR is an ion pump that specifically transports protons [24]. This raises questions regarding the role of each of these enzymes, especially since NQR
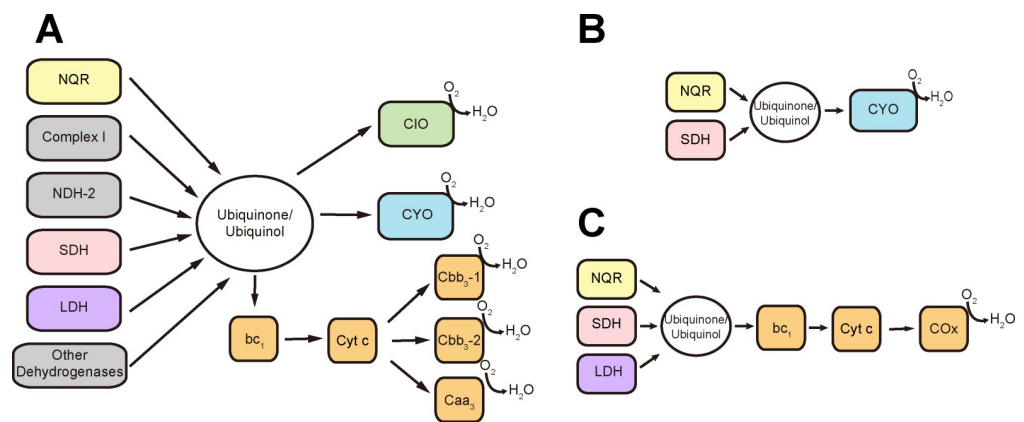

Fig 1. *P. aeruginosa* aerobic respiratory chain. A) Respiratory enzymes annotated in *P. aeruginosa* genome. Main components of the respiratory chain in LB (B) and mAUM (C) media.

and complex I appear to be functionally redundant, and NDH-2 does not participate directly in ion-gradient formation coupled to ATP synthesis. In other bacteria, the respiratory chain typically contains NDH-2 and either complex I or NQR [23,25–27], and the presence of all three NADH dehydrogenases is quite uncommon.

Although many studies have addressed the role of different respiratory complexes through mutagenesis, transcriptomics and genomics tools [13,28–32], a clear picture of how these complexes participate in the respiratory chain is currently unavailable. In this work, we performed systematic functional and kinetic characterizations of the aerobic respiratory chain of *P. aeruginosa* cultured in Luria Broth (LB) and modified artificial urine medium (mAUM), to understand the composition of the respiratory chain and its physiological role in cells growing in conditions that resemble urine. Our results indicate that *P. aeruginosa* respiratory chain composition is deeply influenced by the environmental conditions, which could be advantageous for its survival and could be important to establish a successful infection. For instance, while cytochrome CYO oxidase plays a major role in LB medium, the COx's terminal oxidases play a dominant role in mAUM. Our results also show that NQR is the most important NADH dehydrogenase in both conditions. These studies are important to better understand the physiology of this important pathogenic bacterium and the role of the respiratory complexes in the survival in the urinary tract and in the initial steps of the colonization process, which may allow the identification of new therapeutic targets against *P. aeruginosa*.

Materials and methods

Modified artificial urine medium

The growth medium used in this study to simulate urine is a modification of the Artificial Urine Media reported by Brooks and Keevil [33]. The modifications are found in Table 1. One of the

Table 1. Comparison of artificial urine and modified artificial urine media.

	[Nutrient]	
	AUM	**mAUM**
EDTA	-	3 mM
Citric acid	2 mM	2 mM
$CaCl_2$	2.5 mM	2.5 mM
NaCl	90 mM	80 mM
Na_2SO_4	10 mM	10 mM
$MgSO_4$	2 mM	-
$MgCl_2$	-	5 mM
KH_2PO_4	7 mM	50 mM
K_2HPO_4	7 mM	-
Uric acid	0.4 mM	0.23 mM
$NaHCO_3$	25 mM	37 mM
Peptone L37	1 (g/l)	-
Bovine peptone	-	1 (g/l)
Yeast extract	0.5 (g/L)	0.5 (g/L)
Urea	170 mM	170 mM
Creatinine	7 mM	7 mM
NH_4Cl	25 mM	25 mM
Lactic acid/ Sodium lactate	1 mM	1 mM
$FeSO_4$	5 μM	3.5 μM
pH	6.5	6.5

problems that we encountered with the original protocol is that precipitates were easily formed. Indeed, the authors indicate that precipitations were formed in AUM at temperatures higher than 25°C, which does not allow us to explore physiologic temperatures. Precipitation in mAUM was eliminated by adding 3 mM EDTA to the solution and by using $MgCl_2$ instead of $MgSO_4$. EDTA has shown antibacterial effects against *P. aeruginosa* planktonic cells and biofilms. However, these effects are blocked completely in the presence of calcium and iron [34]. As shown in Table 1, mAUM contains a molar excess of calcium, magnesium and iron compared to EDTA. Analysis of species concentrations using Chelator [35] indicates that the concentration of free EDTA is negligible in this medium, consistent with the healthy cell growth in these conditions. The concentration of phosphate was increased to 50 mM to serve as buffer, as the pH of the original medium spontaneously increased a few hours after preparation, probably due to the chemical decomposition of urea into ammonium. Finally, the concentration of uric acid was decreased to 0.23 mM, below its solubility limit (0.4 mM; 68 mg/ L) but within physiologic concentrations [36]. With these modifications we obtained a stable and reproducible medium that sustains *P. aeruginosa* growth and allows the study of this microorganism in conditions simulating human urine.

P. aeruginosa growth

Overnight cultures of *P. aeruginosa* PAO1 grown in LB broth media were washed with saline solution (0.9% NaCl). The washed cells were inoculated (1:1000 dilution) into LB broth or mAUM and were grown under agitation (250 rpm) at 37°C. Bacterial growth was monitored by measuring OD_{595}. The growth curves were fitted to a logistic function (Eq 1) [37] to calculate the growth rate (μ), maximum growth (a) and lag phase (l).

$$y = \frac{a}{1 + e^{\frac{4\mu}{a}(l-t)+2}} \tag{1}$$

P. aeruginosa membrane preparation

P. aeruginosa PAO1 cells were harvested at the early stationary phase of growth, washed twice with KHE buffer (150 mM KCl, 20 mM HEPES, 1 mM EDTA, pH 7.5) and stored at -80°C. Frozen cell pellets were thawed, resuspended in KHE buffer supplemented with 10 μg/ ml DNAase I, 5 mM $MgCl_2$ and 1 mM PMSF, and passed twice through an Emulsiflex-C5 high pressure homogenizer (Avestin) at 16,000 psi. Cell debris was eliminated by centrifugation at $10,000 \times g$ for 30 min at 4°C. The supernatant was collected and ultracentrifuged at $100,000 \times g$ for 5 h. The pellet, containing the membranes, was washed and resuspended in KHE buffer and stored at -80°C.

P. aeruginosa NQR purification

P. aeruginosa NQR was purified as described previously [24]. Briefly, *P. aeruginosa* *nqrA-F* NQR operon was cloned in pBAD plasmid and transformed into *Vibrio cholerae* O395N1 *Δnqr* cells [38]. The protein complex was expressed (upon addition of arabinose to the culture media) and was purified from cytoplasmic membranes after solubilization with β-D-dodecyl-maltoside (DDM) and Ni-NTA affinity chromatography, followed by anion exchange chromatography, using DEAE-Sepharose [38]. Protein concentration for these and other samples was measured by the BCA assay. NQR concentration was measured spectrophotometrically at 450 nm in a Gd-Cl denatured sample, as described before [38].

Blue native gel electrophoresis and NADH dehydrogenases in gel activity

Proteins were separated by blue native gel electrophoresis, as described by Schagger *et al.* [39]. Briefly, the membranes were solubilized in buffer containing 750 mM ε-aminocaproic acid, 50

mM Bis-Tris, pH 7 and DDM (2 g/g prot) for 30 min on ice. The suspension was centrifuged at 100,000 x *g* for 40 min and the supernatant, containing the solubilized membrane proteins, was collected, mixed with 3x running buffer (with Coomassie blue G-250) and loaded in the gel's well. The samples were resolved in 4–16% polyacrylamide gradient gel. In-gel NADH dehydrogenase activity staining was performed as reported previously [40]. BN-PAGE gel lanes were sliced and incubated at room temperature in buffer containing 100 mM Tris-HCl, 140 μM NADH, 50 μM MTT, pH 7.4. After activity staining, the excess of background Coomassie blue was removed by washing the gel in 0.1% SDS.

Second dimension SDS- PAGE

BN-PAGE bands containing NADH dehydrogenase activity were excised and incubated for 30 min in 60 mM Tris-HCl, pH 6.8, 1% SDS, 1% β-mercaptoethanol. The gel pieces were washed twice with 25 mM Tris, 192 mM glycine, 0.1% SDS and then mounted on a 15%-SDS-PAGE. The gel was exposed to UV light to identify the fluorescent bands corresponding to NQR subunits C and B containing the covalently-bound FMN [41]. The gel was then stained with Coomassie blue.

Oximetry

The respiratory activity of *P. aeruginosa* membranes (0.2 mg of protein /mL) was measured at 37˚C in KHE buffer in a 2 mL custom-made glass chamber, adapted to a Clark-type oxygen electrode (YSI 5300), as described previously [42]. Assays were carried out in the presence of specific substrates and inhibitors for each of the respiratory complexes. NADH oxidase activity was tested using 200 μM NADH. Succinate dehydrogenase was tested in presence of 20 mM succinate. The activity of other dehydrogenases was measured with 10 mM D, L- malate, 10 mM L-lactate, 10 mM glucose or 0.3% ethanol. Quinol oxidase activity was assessed with 50 μM ubiquinone-1 (2,3-Dimethoxy-5-methyl-6-(3-methyl-2-butenyl)-1,4-benzoquinone, Sigma-Aldrich) or menaquinone-2 (2-(3,7-dimethyl-2,6-octadienyl)-3-methyl-1,4-Naphthoquinone, Sigma-Aldrich) in the presence of 500 μM DTT, which readily reduces these quinones [43–46]. The activity of cytochrome *c* oxidases was tested with the artificial redox couple 100 μM TMPD$^+$ and 5 mM ascorbic acid.

KCN titration analysis

The NADH-dependent respiratory activity of the two types of membranes was measured in the presence of different concentrations of KCN, freshly prepared in KHE buffer. Initial activity rates were plotted against KCN concentrations and the data was fitted to the equation of three independent enzymes competitively inhibited by KCN. The equation for each of these enzymes has the familiar form: $v = Vmax$ ([S]/Km)/ (1 + ([S]/ Km) + ([I]/ K_{iapp}), where $Vmax$ is the maximum activity of the enzyme, K_{iapp} is the apparent inhibition constant and [S]/ Km is the substrate's saturation ratio (assumed to be close to saturating, >10).

NADH dehydrogenase activity

P. aeruginosa membranes were solubilized with 0.3% DDM for 30 min at 4˚C and the suspension was ultracentifuged at 100,000 x *g* for 1 h. The supernatant was used to measure the NADH-dependent ubiquinone reduction at 282 nm [38] in KHE buffer containing 50 μM ubiquinone-1 and 250 μM NADH or 250 μM deamino NADH.

Results

P. aeruginosa growth in LB and mAUM

P. aeruginosa PAO1 strain was cultured aerobically in modified artificial urine media (mAUM) (see Materials and Methods), to simulate the conditions that the planktonic state of this microorganism might encounter in the urinary tract or in catheters when they start the colonization process. Previous studies showed that the urinary tract environment is aerobic, with urine's oxygen concentration ranging from 130 to 90 μM in healthy patients *vs* patients with urinary tract infections [47]. Moreover, the microorganisms associated with these infections are aerobic or microaerophilic [48]. However, some studies indicate that in certain conditions urinary tract infections could be microaerophilic [49,50].

mAUM medium is based on the previously published AUM [33] with some modifications to improve the solubility of salts, reduce precipitations and drastic changes in pH (Table 1, see Materials and Methods). The bacterial growth obtained in mAUM (Fig 2B) was compared to the growth in standard laboratory Luria Broth medium (Fig 2A). *P. aeruginosa* growth curves were analyzed using a logistic function (Eq 1, Materials and Methods) [37]. The main parameters obtained from this analysis are the duplication rate (μ) (Fig 2C), total growth (a) (Fig 2D) and length of the lag phase (l) (Fig 2E). Although significant differences were found in all three parameters, the major changes were found in the growth rate and total growth, which were 3 and 7 times higher in LB media *vs* mAUM, respectively. Due to the changes in growth kinetics, the stationary phase was reached at 15 h in LB (Fig 2A) and at 6 h in mAUM (Fig 2B). The growth rates in LB reported here are similar to the growth rates reported in other works [31]. Importantly, these data indicate that *P. aeruginosa* actively grows in these conditions and does not enter a dormant state or immediately produces biofilms when exposed to urine.

Organization of *P. aeruginosa* respiratory chain in mAUM *vs* LB media: Dehydrogenases and quinones

To understand the metabolic adaptations of *P. aeruginosa* in conditions that mimic human urine, cells were cultured in mAUM and LB media and harvested at the early stationary phase
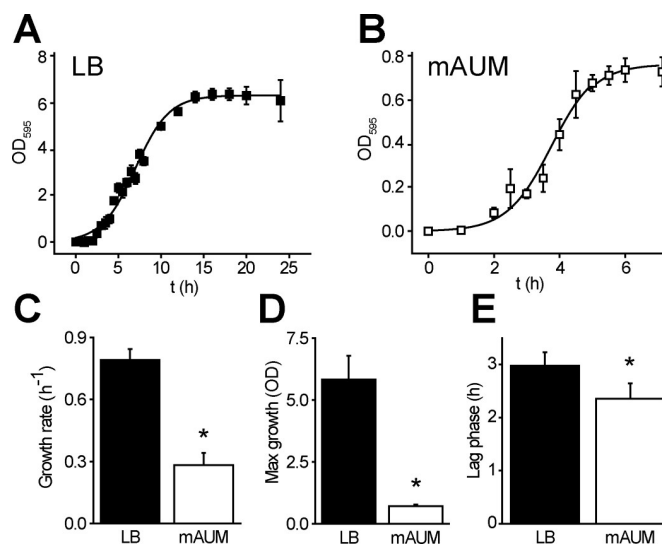

Fig 2. *P. aeruginosa* growth in LB and mAUM. *P. aeruginosa* growth curves in LB (A) and mAUM (B) media. Comparison of growth parameters between LB and mAUM: growth rate (C), maximum growth (D) and lag phase (E). These parameters were calculated using Eq 1. Results are expressed as mean ± S.D. n ≥ 5. *, p<0.01 after t test.

of growth. To characterize the aerobic respiratory chain, oxygen consumption rates (OCR) were measured in purified plasma membranes. OCR activities were measured in the presence of different substrates: NADH, succinate, lactate, malate, glucose and ethanol. Moreover, experiments were carried out with ubiquinol or menaquinol to identify the type of quinone used by the cells. Fig 3A and 3B shows the dehydrogenase activities of *P. aeruginosa* membranes in each growth media. As can be observed, NADH dehydrogenase and succinate dehydrogenase activities are 40–50% smaller in mAUM (Fig 3B) *vs* LB (Fig 3A). Malate dehydrogenase also show differences, with higher activities in LB medium (Fig 3A and 3B). On the other hand, lactate dehydrogenase activity was not modified in these conditions. Glucose oxidase and ethanol dehydrogenases were also tested but have minor activities compared to the other dehydrogenases.

In order to determine the type of quinone used as electron carrier, we tested the respiratory activity in presence of ubiquinol-1 and menaquinol-2. Fig 3 shows that the ubiquinol oxidase activity is similar compared to the NADH dehydrogenase activity in LB (Fig 3A) and mAUM (Fig 3B), while menaquinol oxidase activity is negligible in both types of media. The data indicate that ubiquinone is the preferred electron carrier in the respiratory chain of this bacterium.

Composition of *P. aeruginosa* respiratory chain in mAUM *vs* LB media: Terminal oxidases

As mentioned above, in addition to cytochrome bc_1 and three cytochrome c oxidases (COx), *P. aeruginosa* contains two different ubiquinol oxidases: CIO and CYO [12,28,30]. To understand the role of these complexes in these growth conditions, the respiratory activity obtained with ubiquinol was compared to the rate of oxygen consumption in presence of ascorbic acid and $TMPD^+$. Ascorbate-$TMPD^+$ chemically reduce the endogenous cytochrome c and is used as substrate by COx oxidases [51]. TMPD-ascorbate oxidase activity is 6 and 2 times higher compared to the ubiquinol oxidase activity in LB (Fig 3A) and mAUM (Fig 3B) membranes, respectively. These results could suggest that in both media COx oxidases play a major role. However, these measurements cannot be used to predict the activity *in situ*, since COx activity
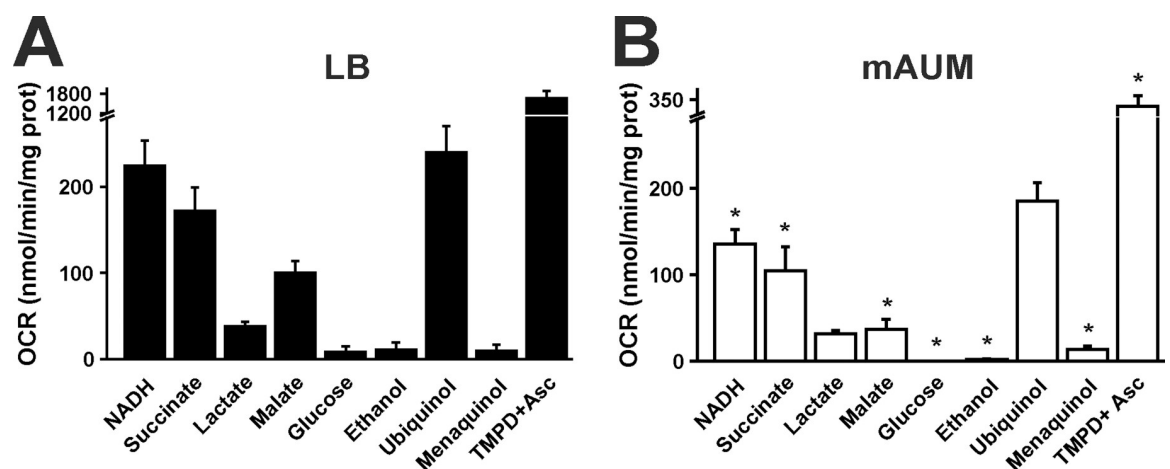

Fig 3. *P. aeruginosa* respiratory activity in LB and mAUM membranes. Oxygen consumption rate (OCR) of membranes obtained from bacteria grown in LB (A) or mAUM (B). Oxygen consumption was measured in KHE buffer in the presence of the next substrates: 200 μM NADH, 10 mM succinate, 10 mM lactate, 10 mM glucose, 0.3% ethanol, 50 μM ubiquinol or 50 μM menaquinol or 100 μM $TMPD^+$ plus 5 mM ascorbic Acid. Bars represent mean ± S.D. n ≥ 3. *, p<0.05 after t test between LB and mAUM.

https://doi.org/10.1371/journal.pone.0231965.g003

was assayed by fully-reducing cytochrome c (representing near-maximal activities) and reduced cytochrome c concentration could be far from optimal under physiologic conditions.

To measure the relative contribution of the three types of oxidases to cell physiology, the respiratory activity was measured in the presence of different concentrations of KCN. The terminal oxidases have very different cyanide sensitivities, which can be used as a tool to quantify their relative contributions to respiration. As shown in Fig 4, the KCN titration of the NADH-dependent respiratory activity revealed three distinct kinetic components for LB (Fig 4A) and mAUM (Fig 4B) membranes, with apparent inhibition constants (Ki_{app}) that were at least one order of magnitude higher, producing step ladder-like curves. The first component is highly sensitive to cyanide, with a Ki_{app} of 0.5–1 μM, consistent with the high affinity of COx oxidases for this inhibitor [52,53], including those of *Pseudomonas* species [54]. The second component has a Ki_{app} of 10 μM, similar to the reported values for CYO oxidase (8 μM) [55,56]. The last component has a Ki_{app} of 2.5 mM, and it is most likely due to CIO oxidase activity, which is highly resistant to cyanide [32,56]. To corroborate that *P. aeruginosa* terminal oxidases have similar sensitivities for cyanide as other members of these families, we carried out a KCN titration of the COx and ubiquinol oxidases in LB membranes (Fig 4D and 4E). COx activity was measured using Ascorbate-TMPD, as described previously. Fig 4D shows that the COx activity is highly sensitive to KCN, with a K_{iapp} of 0.3±.1 μM, which corroborates that the first kinetic component in Fig 4A (magnified in the Fig 4D inset) is indeed COx. Ubiquinol oxidase activity
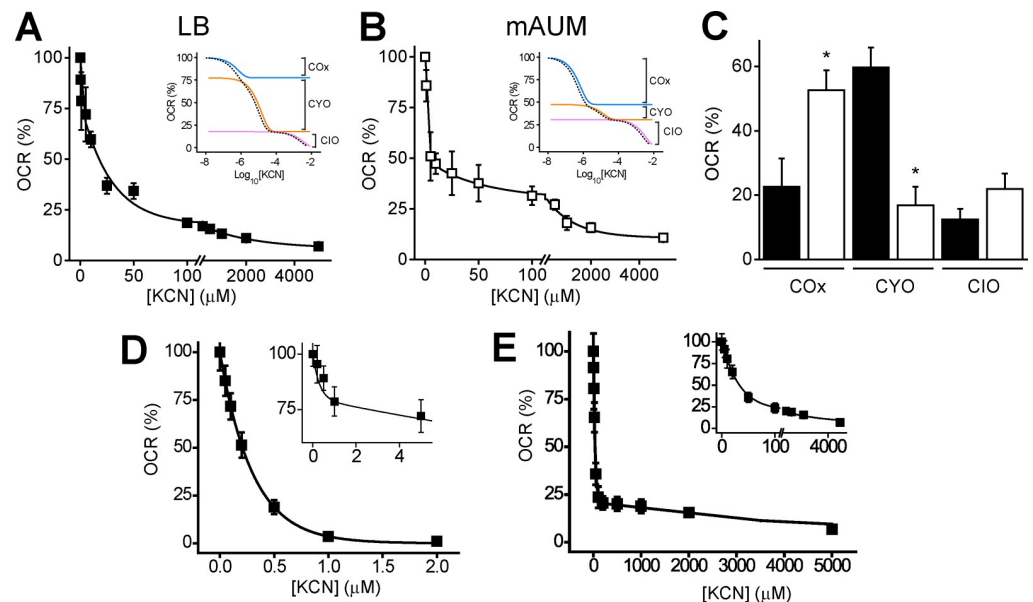

Fig 4. Cyanide titration of respiratory activity. NADH-dependent respiratory activities were measured in LB (A) and mAUM (B) membranes in the presence of different concentrations of KCN (0–5 mM). Titration curves were fitted to the function with three independent Competitive Inhibition Michaelis-Menten components (see Materials and Methods). The first component (K_{iapp}<1 μM) was assigned as COx, the second component (K_{iapp} 10 μM) was assigned as CYO and the third component (K_{iapp} 2.5 mM) was assigned as CIO. The activities (*Vmax*) of these components in LB (black bar) and mAUM (white bar) are compared in panel C. Bars represent mean ± S.D. n ≥ 3. *, p<0.01 after t test. Insets in panels A and B show the expected titration curves of COx (blue), CYO (orange) and CIO (pink) oxidases, and the addition of the three components (dashed black line). The colored lines were slightly moved to the right for clarity. D) Titration of the Ascorbate /TMPD respiratory activity of LB membranes. The fitting line was obtained with a single-component kinetic model. The inset shows a magnification into the 0–5 μM KCN region of panel A. E) KCN titration of the ubiquinol-dependent respiratory activity in the presence of 1 μM antimycin A, which inhibits cytochrome bc_1. The fitting line was obtained with a two-component kinetic model, with K_{iapp} values of 15 μM and 3 mM. The inset shows a replotting of the data with a break from 100–200 μM KCN.

was measured with ubiquinol- DTT in the presence of 1μM antimycin A, which specifically inhibits complex bc_1 and indirectly inhibits COx. The titration of the activity revealed two components, with K_{iapp}'s of 15 μM and 3 mM, likely corresponding to CYO and CIO.

The triphasic behavior found in Fig 4A and 4B (with similar K_{iapp}'s as found here) has been reported in other species, such as *Pseudomonas pseudoalcaligenes* [54] and it is also evident in the re-plotting of the original data on *P. aeruginosa* respiration by Cunningham, *et al.* [32]. In previous reports cyanide titration data was analyzed using the empirical equation: A/ 1+([I]/ IC_{50})^n [56], which it is not based on a strict kinetic model and incorporates a "Hill coefficient" (n), providing a seemingly good data fitting but no strict biochemical meaning. In this report, the titration curves were analyzed with an equation that considers three independent kinetic Michaelis-Menten components, with individual Ki_{app} and *Vmax* values (see Materials and Methods), showing excellent fitting to the data. Insets in Fig 4A and 4B show the predicted activities of each kinetic component when varying the cyanide concentration, to better illustrate the analysis carried out. As can be observed, the first (COx) and the second (CYO) components are saturated by cyanide concentrations of 10 and 100 μM, while and the third component (CIO) is active at concentrations in the mM range. Fig 4C shows the comparison of the activities (*Vmax*) of the three components, as can be observed the three types of oxidases have significant contributions to the respiratory activity in both cases. However, the relative contribution of each oxidase varies depending on the culture medium. In LB medium 50% of the activity can be attributed to CYO oxidase, while in mAUM more than 60% of the activity can be attributed to COx. This difference could be related to the importance of energy balance in the relatively poorer urine medium (see below).

Composition of *P. aeruginosa* respiratory chain in mAUM *vs* LB media: Role of NADH dehydrogenases

Three different NADH dehydrogenases are annotated in the genome of *P. aeruginosa*: complex I, NDH-2 and NQR. The presence of the three types of NADH dehydrogenases is puzzling, especially since NQR and complex I are both proton pumps [24,57] and NDH-2 is not linked to the generation of an electrochemical gradient. Here we aim to elucidate the roles of these enzymes in the physiology of *P. aeruginosa*. Although these enzymes catalyze the same redox reaction, they can be distinguished by their molecular weights, using blue native gel electrophoresis (BN-PAGE), and by their inhibitor sensitivity and substrate specificity. Membranes of cells grown in LB and mAUM were solubilized using n-dodecyl-β-D-maltoside (DDM) (2 g /g prot). The proteins were separated using BN-PAGE and the NADH dehydrogenase activity was assayed in-gel, using NADH as substrate and MTT (3-(4,5-dimethylthiazol-2-yl)-2,5-diphenyl-tetrazolium bromide) as an artificial electron acceptor. The reduction of MTT produces a formazan precipitate and purple bands appear in the gel in locations where the NADH dehydrogenase reaction takes place. Two NADH dehydrogenase bands of 100 and 220 kDa (Fig 5B) were observed in both types of membranes, matching the molecular weights of a NDH-2 dimer (46 kDa monomer) and the six-subunit NQR complex (210 kDa) [24]. To estimate the relative activity of both bands, the reaction was measured densitometrically at different time points (Inset Fig 5B). From the initial rates we determined that the 220 kDa band is 3–5 times more active than the 100 kDa band. A third band, with an estimated molecular weight of 500 kDa (likely corresponding to complex I [16,23]), could also be observed in LB membranes, but the incubation time required to visualize this band was much longer (overnight) compared to the other bands. The 220 kDa BN-PAGE bands were excised and ran in a second dimension SDS-PAGE. The gel was exposed to UV light a fluorescent bands were observed in the lanes of the 220 kDa complex, corresponding to the covalently-attached FMN to subunits B and C of
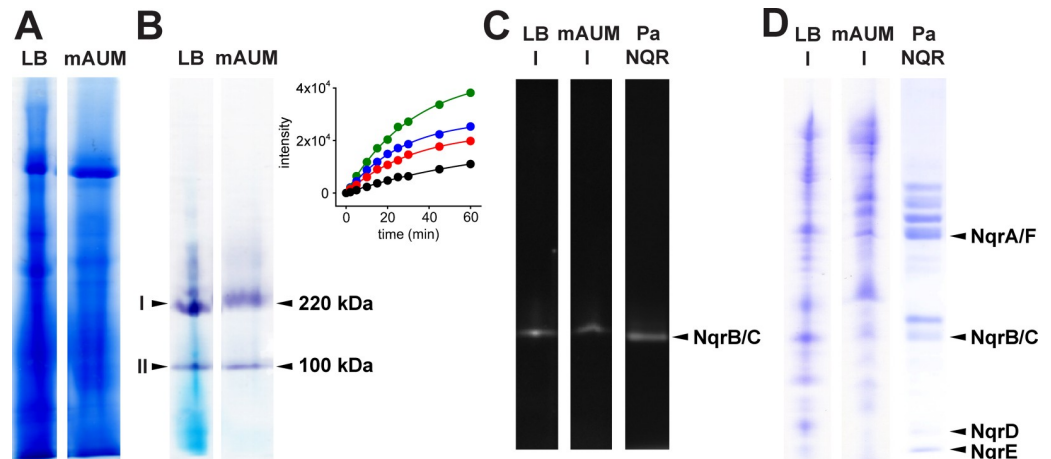
Fig 5. BN and 2D-SDS PAGE identification of NQR in LB and mAUM membranes. A) Coomassie-stained BN-PAGE gel of lanes containing solubilized LB and mAUM membranes. B) In-gel NADH dehydrogenase activity of BN-PAGE lanes of LB and AUM membranes, showing the 100 and 220 kDa bands. Inset, densitometry assay of the in-gel kinetics of NADH dehydrogenase activity (Black, LB -100 kDa; Red, AUM-100 kDa; Blue, LB-220 kDa; Green, AUM-220 kDa). The 220 kDa bands of the BN-PAGE gel were excised and run in a second dimension SDS-PAGE. The 2D gel lanes were exposed to UV light to identify the fluorescent bands of NQR subunits B and C (panel C), which co-migrate in this type of gel, due to the high hydrophobicity of subunit B, and were subsequently Coomassie-stained (D). Purified Pa-NQR [24] was run as standard for comparison.

NQR (Fig 5C) [41,58], as confirmed by mass spectrometry analysis (Proteomics Unit, University of Illinois at Chicago) of the fluorescent band (S1 Table). The 220 kDa band also contain the six subunits of the NQR complex, as shown in the Coommassie-stained 2D SDS-PAGE gel (Fig 5D), confirming the presence of this enzyme in both conditions.

The 2D-SDS PAGE of the 100 kDa band contained a band with the expected molecular weight of NDH-2 of 46 kDa, which was excised and analyzed by mass spectrometry. Several proteins were identified but none of them corresponded to NDH-2 (S1 Table). Although the 100 kDa band has significant activity in gel, it is not related to any enzyme of the respiratory chain. It should be pointed out that the turnover rates of NQR (500 s^{-1} [38]) and NDH-2 (900 s^{-1} [59]) are comparable and based on NQR abundance in the gel, NDH-2 should be an abundant band as well, if the 100 kDa activity band contains this protein.

Although in-gel activity measurements indicate that NQR is the main NADH dehydrogenase, the effects of specific inhibitors of complex I (rotenone) [60] and NQR (HQNO, N-2-heptyl-4-hydroxyquinoline) [61,62] were tested on the rate of oxygen consumption in membranes obtained from LB or mAUM media to confirm this hypothesis. At a saturating concentration, rotenone (1 μM) (K_i = 4 nM) [63,64] inhibits <20% of the respiratory activity of LB membranes (Fig 6A), and had no effects on the activity of mAUM membranes (Fig 6B), indicating that complex I does not participate in the respiratory activity in mAUM, consistent with the low activity obtained in in-gel assays. The titration of the NADH-dependent activity with HQNO produced a curve with a K_i = 2 μM and a kinetic component of 40% that is insensitive to concentrations >10 μM of this inhibitor, in both types of membranes (Fig 6C and 6D). This behavior is nearly identical to the titration of the purified *P. aeruginosa* NQR (Fig 6C inset) [24]. To test that HQNO and rotenone act specifically on the NADH dehydrogenases, these inhibitors were tested using succinate as a substrate, as it has been reported that HQNO can inhibit other respiratory enzymes [65–67]. As shown in Fig 6A and 6B, the inhibitors had little effect on the activity with succinate in both types of membranes, indicating that at these concentrations they act specifically on the NADH dehydrogenases, in particular on NQR.
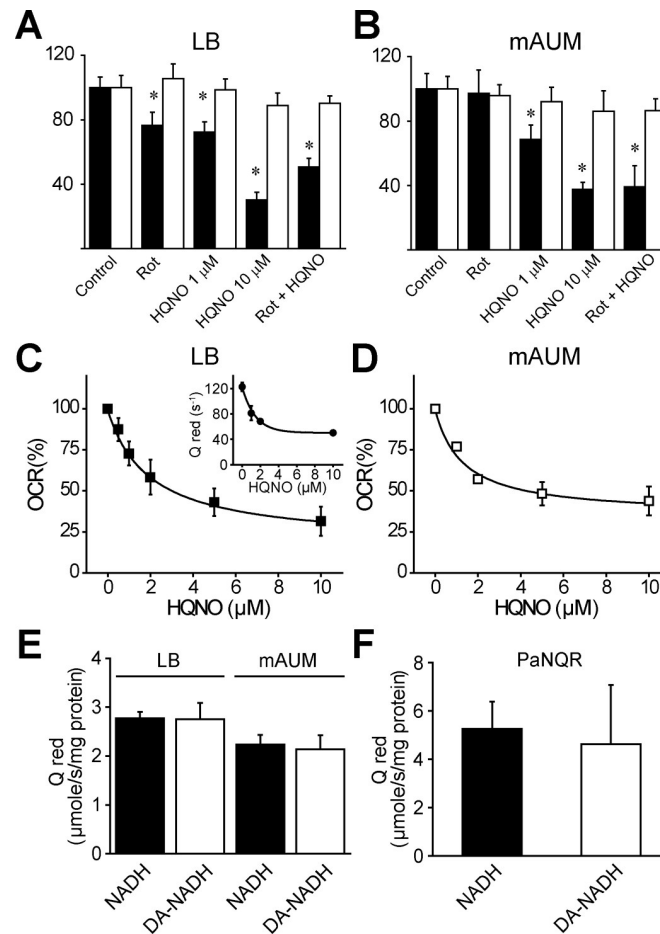
Fig 6. NQR activity measurements in LB and mAUM membranes. NADH-dependent (black) and Succinate-dependent respiratory activity of LB (A) or mAUM (B) membranes in the presence of rotenone (1 μM) or HQNO (1 or 10 μM). Bars represent mean ± S.D. n ≥ 3. *, p<0.05 after t test between NADH-dependent (black) or Succinate-dependent (white) respiratory activity. Effect of HQNO on the NADH-dependent rate of oxygen consumption in LB (C) and mAUM membranes (B). Inset in C, HQNO titration on the activity of the purified Pa-NQR. Inset data were taken from reference [24]. Ubiquinone reductase activity of solubilized membranes obtained from cells grown in LB or mAUM (E) or purified *P. aeruginosa* NQR (F) using as substrates NADH (black) or deamino NADH (white; DA-NADH). Data are expressed as SDM (n ≥ 5). * p < 0.05 vs control.

Finally, to corroborate that the NADH-dependent respiratory activity in membranes is mostly due to NQR and not to NDH-2, we tested the ubiquinone oxidoreductase activity in membranes solubilized with DDM using NADH or diamino-NADH as substrates. While NQR can use both substrates equally well (Fig 6F) [68,69], NDH-2 can only use NADH [70,71]. The ratio of activity with NADH and deamino-NADH can be used to determine the contributions of these two enzymes. As shown in Fig 6E, the activities obtained with these two substrates are nearly identical in both types of membranes. Taken together the data unambiguously demonstrate that NQR is the main NADH dehydrogenase for *P. aeruginosa* in the conditions tested in this study.

Discussion

Previous studies using proteomics, transcriptomic and mutagenesis methodologies have addressed the role of different respiratory complexes for this microorganism [13,28–32].

However, these methodologies have intrinsic limitations and a clear understanding of the specific roles of respiratory enzymes used by *P. aeruginosa* in diverse conditions is missing. Among the aspects that limit the usefulness of these techniques are: 1) transcriptomics studies normally report the relative expression of a gene compared with a specific "basal" condition and mRNA content does not necessarily directly correspond to protein content, 2) proteomic identification and quantification may not be used to estimate the enzymatic activity in the pathway, due in part to the presence of inactive and active pools of enzymes (apo vs holo) and because protein content does not necessarily linearly correlate with enzymatic activity, due to multifactorial regulation. On the other hand, mutagenesis studies are a powerful tool to analyze the effects of gene elimination on microbial growth parameters. However, this technique relies on the ability of cells to grow in the absence of specific genes, and it is highly likely that this method could select variants that can withstand genetic manipulation by upregulating other genes or pathways, which might not represent the wild-type genetic background. In this report we performed a comprehensive functional characterization of the respiratory chain of *P. aeruginosa*, measuring directly the metabolic and enzymatic activities within their pathways. Although the method is disruptive to the cell, it allows the direct determination of the activities of different respiratory complexes using their specific kinetic properties, including substrate and inhibitor specificity. Our results allow us to reconstruct the electron transfer pathway used by *P. aeruginosa* planktonic state while growing in medium similar to human urine.

Role of succinate dehydrogenase, malate dehydrogenase and lactate dehydrogenase in carbon flux

Previous studies have shown that the Krebs and glyoxylate cycles are highly active in *P. aeruginosa* isolated from both cystic fibrosis patients and from urinary tract infections [72]. Here we have found that succinate dehydrogenase is very active in both LB and mAUM membranes, which is consistent with a high carbon flux through these pathways, allowing the synthesis of important molecules for bacterial survival [72]. In addition, we report an important respiratory activity with malate in both LB and mAUM membranes, which indicates that the membrane-bound malate dehydrogenase [73] found in the genome is active. *P. aeruginosa* genome also contains two genes for membrane-bound lactate dehydrogenases (mLDH), which transfer the electrons to ubiquinone, rather than to NAD as the soluble enzyme does [74]. The relatively high activity of mLDH found in mAUM membranes could be advantageous for the growth in urine medium, which contains high amounts of the racemic mixture of lactate, the products of human (L-lactate) and microbial metabolism (D-lactate) [75].

Role of terminal oxidases in artificial urine medium

Although, P. aeruginosa is an important human pathogen that produces one of the most common hospital-acquired infection, the regulation and physiologic roles of *P. aeruginosa* terminal oxidases during urinary tract infections have remained completely unknown. Previous reports suggested that CYO is not a critical enzyme for the aerobic metabolism of *P. aeruginosa*, since its expression is low in LB medium and it seems to be induced specifically during iron starvation [76]. Moreover, mutants that lack this enzyme do not show major changes in the growth parameters [28]. However, our results unambiguously indicate that CYO is the main terminal oxidase in LB medium, contributing to 50% of the respiratory activity. These findings highlight the need to complement mutagenesis, proteomic and transcriptomic data with functional analysis of the enzymes and metabolic pathways. Interestingly, in other gram-negative proteobacteria, such as the closely-related *Pseudomonas putida* [77], and also in *Escherichia coli* [78] as

well as in *Gluconobacter oxydans* [79], CYO was also found to be the main terminal oxidase, suggesting a common evolutionary or physiologic trend among prokaryotes.

On the other hand, in mAUM membranes 60% of the activity can be attributed to COx oxidases, since most of the activity is sensitive to very low cyanide concentrations ($< 1\mu M$). Among the three different types of terminal oxidases, COx oxidases (caa_3, cbb_3-1 and cbb_3-2) provide the highest energy yields to the cell. COx oxidases could be favored in mAUM because it is not a rich medium compared to LB and in these conditions cell energetics could have a predominant role. Cytochrome cbb_3-1 oxidase may be the main terminal oxidase used in these conditions, since it is constitutively expressed and appears to be a major component during exponential growth. On the other hand, cbb_3-2 oxidase appears to be induced in the stationary phase when the oxygen tension drops [80] and previous studies have shown that caa_3 oxidase expression is extremely low under aerobic conditions [76]. Recent studies have shown that cbb_3 oxidases are important for the formation of biofilms by *P. aeruginosa*, which strongly suggests that this terminal oxidase plays major roles during the colonization of lung epithelium [81] and as shown in this work, also in the colonization of the urinary tract or catheters. As shown in Fig 4, both types of membranes have a significant cyanide-resistant respiratory activity, which can be attributed to CIO oxidase [12,82–84]. CIO oxidase expression has been considered a pathogenicity marker for *P. aeruginosa* [82], since this microorganism actively produces cyanide during infection [28], which can be as high as 300 μM in culture [32].

Role of NQR in *P. aeruginosa* physiology: Autopoisoning resistance

Recent studies show an increased expression of complex I and NQR in *P. aeruginosa* isolated from cystic fibrosis patients [85]. Moreover, mutagenesis analyses indicate that complex I is critical for the survival of *P. aeruginosa* under microaerophilic conditions [15,86]. However, the role of NADH dehydrogenases in the physiology and pathogenic behavior of this bacterium remains almost completely unknown. In this work we have determined that *P. aeruginosa* NADH dehydrogenase is highly active in LB and mAUM. In both media most of the NADH dehydrogenase activity is resistant to rotenone, indicating that complex I does not play a major role in the respiratory activity. To test if NQR or NDH-2 are functional in these conditions, a titration with HQNO was performed. Although, the titration curve of the respiratory chain is almost identical to the titration of isolated NQR [24] (Fig 6C), HQNO can also inhibit NDH-2 [65,67,87]. To distinguish between NDH-2 and NQR, the activity was measured with NADH and deamino-NADH. While NQR can use both substrates, NDH-2 is inactive with deamino NADH. The data indicate that the NADH dehydrogenase activity is nearly identical with both substrates, clearly demonstrating that NQR is the main NADH dehydrogenase in *P. aeruginosa*. These results are consistent with the BN-PAGE band of 220 kDa having the greatest activity, which contains the six NQR subunits, including the fluorescent subunits B and D. Although the 100 kDa band also has significant NADH dehydrogenase activity, it did not contain NDH-2 and the activity could be due to other flavoproteins present in the sample.

In a recent report, Torres, *et al.* [15] showed that *P. aeruginosa* mutants lacking complex I are unable to grow under anaerobic conditions, are less sensitive to gentamycin and showed slightly reduced virulence compared to the wild-type strain, which might indicate that this respiratory complex plays a major role. This conclusion contrasts sharply with the lack of effect of rotenone in our experiments. Interestingly, the authors also showed that individual mutants of complex I, NDH-2 and NQR had no effects on the growth kinetics in several types of growth media, including LB. These results were confirmed by our group, using selected *P. aeruginosa* P14 mutant library strains (kindly provided by Dr. Martin Schuster, Oregon State University [88]). As indicated above, mutagenesis studies report the tolerance of microorganisms to the

lack of specific enzymes. In the case of *P. aeruginosa*, it is not surprising that the other two NADH dehydrogenases can compensate for the lack of any individual enzyme, especially since the cells can grow aerobically even when all three dehydrogenases are removed [15]. Our results show unambiguously that NQR is the preferred NADH dehydrogenase for *P. aeruginosa* in the tested conditions, but as shown by the mutagenesis analysis, it is not an essential enzyme.

These results and a recent report by our group [24] suggest that the respiratory chain of *P. aeruginosa* has evolved with the ability to resist auto-poisoning. We previously demonstrated that *P. aeruginosa* NQR is resistant to HQNO, and that the resistance is conferred by residues Leu151 and Phe155 located in subunit D of the ubiquinone binding site [24]. This characteristic could be an advantage to avoid autopoisoning, since this microorganism actively produces HQNO to eliminate competing bacteria [66,89,90]. Moreover, in a previous report we proposed that NQR could be important for pathogenic bacteria when iron is limiting [91], which is relevant for the infection since the immune system produces iron chelators that deprive pathogens of this essential nutrient. NQR is the ion-pumping NADH dehydrogenase that requires the least amount of iron for its assembly (1 or 2 atoms per molecule [20,21,92,93]), which could allow an active bioenergetic metabolism and cell survival during infection, in particular when the immune response has been mounted.

The main conclusions of this paper are summarized in Fig 1, showing that NQR is the main NADH dehydrogenase in LB (Fig 1B) and mAUM (Fig 1C), that succinate dehydrogenase also plays a major role and that the main terminal oxidases used by *P. aeruginosa* are CYO and COx in LB and mAUM media, respectively. Our data offers a clear understanding of the organization of the respiratory chain in physiologically relevant conditions and suggests that the apparent redundancy in the number and type of dehydrogenases and oxidases could be an advantage that allows the cells to avoid autopoisoning by HQNO and cyanide, which *P. aeruginosa* actively produces to inhibit the respiratory enzymes of the human host and of competitor bacteria [51,52,97,61,66,67,89,90,94–96, 97].

Supporting information

S1 Table. Proteins identified in the 30 and 46 kDa of the 2D- PAGE gel of LB and mAUM membranes. The 30 kDa fluorescent band was obtained after running a second dimension (2D SDS PAGE) of the 200 kDa band obtained after BN PAGE that contained NADH dehydrogenase activity. The 46 kDa band was obtained after running a second dimension (2D SDS PAGE) of the 100 kDa band obtained after BN PAGE that contained NADH dehydrogenase activity.
(DOCX)

S1 Fig.
(TIF)

Author Contributions

Conceptualization: Dakota C. Bunn, Monica Rosas-Lemus, Claudia C. Häse, Oscar Juárez.

Data curation: Karina Tuz.

Formal analysis: Karina Tuz, Oscar Juárez.

Funding acquisition: Oscar Juárez.

Investigation: Pingdong Liang, Xuan Fang, Yuyao Hu, Ming Yuan, Daniel A. Raba, Jie Ding, Dakota C. Bunn, Krithica Sanjana, Jun Yang.

Methodology: Xuan Fang, Daniel A. Raba.

Project administration: Karina Tuz, Oscar Juárez.

Resources: Claudia C. Häse, Oscar Juárez.

Supervision: Karina Tuz, Oscar Juárez.

Writing – original draft: Pingdong Liang, Xuan Fang, Ming Yuan, Claudia C. Häse, Karina Tuz, Oscar Juárez.

Writing – review & editing: Pingdong Liang, Xuan Fang, Ming Yuan, Claudia C. Häse, Karina Tuz, Oscar Juárez.

References

1. Wiehlmann L, Wagner G, Cramer N, Siebert B, Gudowius P, Morales G, et al. Population structure of Pseudomonas aeruginosa. Proc Natl Acad Sci U S A. 2007; 104: 8101–6. https://doi.org/10.1073/pnas.0609213104 PMID: 17468398

2. Hardalo C, Edberg SC. Pseudomonas aeruginosa: assessment of risk from drinking water. Crit Rev Microbiol. 1997; 23: 47–75. https://doi.org/10.3109/10408419709115130 PMID: 9097014

3. Silver S. Pseudomonas aeruginosa as an opportunistic pathogen. Trends Microbiol. 2003; 2: 33. https://doi.org/10.1016/0966-842x(94)90345-x

4. Williams HD, Zlosnik JEA, Ryall B. Oxygen, Cyanide and Energy Generation in the Cystic Fibrosis Pathogen Pseudomonas aeruginosa BT—Advances in microbial physiology Vol. 52. In: Poole Robert K., editor. Advances in microbial physiology Vol 52. Academic Press; 2006. pp. 1–71. Available: http://linkinghub.elsevier.com/retrieve/pii/S0065291106520016%5Cnpapers3://publication/doi/10.1016/S0065-2911(06)52001-6

5. Lyczak JB, Cannon CL, Pier GB. Lung infections associated with cystic fibrosis. Clin Microbiol Rev. 2002; 15: 194–222. https://doi.org/10.1128/CMR.15.2.194-222.2002 PMID: 11932230

6. Kim YJ, Jun YH, Kim YR, Park KG, Park YJ, Kang JY, et al. Risk factors for mortality in patients with Pseudomonas aeruginosa bacteremia; retrospective study of impact of combination antimicrobial therapy. BMC Infect Dis. 2014; 14: 161. https://doi.org/10.1186/1471-2334-14-161 PMID: 24655422

7. Mittal R, Aggarwal S, Sharma S, Chhibber S, Harjai K. Urinary tract infections caused by Pseudomonas aeruginosa: A minireview. J Infect Public Health. 2009; 2: 101–111. https://doi.org/10.1016/j.jiph.2009.08.003 PMID: 20701869

8. Warren JW. Catheter-associated urinary tract infections. Int J Antimicrob Agents. 2001; 17: 299–303. https://doi.org/10.1016/s0924-8579(00)00359-9 PMID: 11295412

9. Knols BG, Smallegange RC, Tacconelli E, Magrini N, Kahlmeter G, Singh N. Global Priority List Of Antibiotic-Resistant Bacteria To Guide Research, Discovery, And Development Of New Antibiotics. Lancet Infect Dis. 2009; 9: 535–536. https://doi.org/10.1016/S1473-3099(09)70222-1

10. Toyofuku M, Nomura N, Kuno E, Tashiro Y, Nakajima T, Uchiyama H. Influence of the Pseudomonas quinolone signal on denitrification in Pseudomonas aeruginosa. J Bacteriol. 2008; 190: 7947–7956. https://doi.org/10.1128/JB.00968-08 PMID: 18931133

11. Alvarez-Ortega C, Harwood CS. Responses of Pseudomonas aeruginosa to low oxygen indicate that growth in the cystic fibrosis lung is by aerobic respiration. Mol Microbiol. 2007; 65: 153–165. https://doi.org/10.1111/j.1365-2958.2007.05772.x PMID: 17581126

12. Arai H. Regulation and function of versatile aerobic and anaerobic respiratory metabolism in Pseudomonas aeruginosa. Front Microbiol. 2011; 2: 103. https://doi.org/10.3389/fmicb.2011.00103 PMID: 21833336

13. Stover CK, Pham XQ, Erwin AL, Mizoguchi SD, Warrener P, Hickey MJ, et al. Complete genome sequence of Pseudomonas aeruginosa PAO1, an opportunistic pathogen. Nature. 2000; 406: 959–964. https://doi.org/10.1038/35023079 PMID: 10984043

14. Giuffrè A, Borisov VB, Arese M, Sarti P, Forte E. Cytochrome bd oxidase and bacterial tolerance to oxidative and nitrosative stress. Biochim Biophys Acta—Bioenerg. 2014; 1837: 1178–1187. https://doi.org/10.1016/j.bbabio.2014.01.016 PMID: 24486503

15. Torres A, Kasturiarachi N, DuPont M, Cooper VS, Bomberger J, Zemke A. NADH Dehydrogenases in Pseudomonas aeruginosa Growth and Virulence. Front Microbiol. 2019; 10: 75. https://doi.org/10.3389/fmicb.2019.00075 PMID: 30804898

16. Yagi T, Yano T, Di Bernardo S, Matsuno-Yagi A. Procaryotic complex I (NDH-1). An overview. Biochim Biophys Acta—Bioenerg. 1998; 1364: 125–133. https://doi.org/10.1016/S0005-2728(98)00023-1

17. Kerscher S, Dröse S, Zickermann V, Brandt U. The three families of respiratory NADH dehydrogenases. Results Probl Cell Differ. 2008; 45: 185–222. https://doi.org/10.1007/400_2007_028 PMID: 17514372

18. Neehaul Y, Juárez O, Barquera B, Hellwig P. Infrared spectroscopic evidence of a redox-dependent conformational change involving ion binding residue NqrB-D397 in the Na+-pumping NADH:quinone oxidoreductase from Vibrio cholerae. Biochemistry. 2013; 52: 3085–3093. https://doi.org/10.1021/bi4000386 PMID: 23566241

19. Juárez O, Nilges MJ, Gillespie P, Cotton J, Barquera B. Riboflavin is an active redox cofactor in the Na + -pumping NADH:quinone oxidoreductase (Na + -NQR) from Vibrio cholerae. J Biol Chem. 2008; 283: 33162–33167. https://doi.org/10.1074/jbc.M806913200 PMID: 18832377

20. Juárez O, Morgan JE, Barquera B. The electron transfer pathway of the Na+-pumping NADH:Quinone oxidoreductase from Vibrio cholerae. J Biol Chem. 2009; 284: 8963–8972. https://doi.org/10.1074/jbc.M809395200 PMID: 19155212

21. Barquera B, Nilges MJ, Morgan JE, Ramirez-Silva L, Zhou W, Gennis RB. Mutagenesis study of the 2Fe-2S center and the FAD binding site of the Na+-translocating NADH:ubiquinone oxidoreductase from Vibrio cholerae. Biochemistry. 2004; 43: 12322–12330. https://doi.org/10.1021/bi048689y PMID: 15379571

22. Juárez O, Barquera B. Insights into the mechanism of electron transfer and sodium translocation of the Na+-pumping NADH:quinone oxidoreductase. Biochim Biophys Acta—Bioenerg. 2012; 1817: 1823–1832. https://doi.org/10.1016/j.bbabio.2012.03.017 PMID: 22465856

23. Yagi T. Bacterial NADH-quinone oxidoreductases. J Bioenerg Biomembr. 1991; 23: 211–225. https://doi.org/10.1007/bf00762218 PMID: 2050655

24. Raba DA, Rosas-Lemus M, Menzer WM, Li C, Fang X, Liang P, et al. Characterization of the Pseudomonas aeruginosa NQR complex, a bacterial proton pump with roles in autopoisoning resistance. J Biol Chem. 2018; 293: 15664–15677. https://doi.org/10.1074/jbc.RA118.003194 PMID: 30135204

25. Poole RK, Cook GM. Redundancy of aerobic respiratory chains in bacteria? Routes, reasons and regulation. Adv Microb Physiol. 2000; 43: 165–224. https://doi.org/10.1016/s0065-2911(00)43005-5 PMID: 10907557

26. Kita K, Konishi K, Anraku Y. Terminal Oxidases of Escherichia coli Aerobic Respiratory Chain. J Biol Chem. 1984; 259: 3368–3374. PMID: 6365921

27. Häse CC, Barquera B. Role of sodium bioenergetics in Vibrio cholerae. Biochim Biophys Acta—Bioenerg. 2001; 1505: 169–178. https://doi.org/10.1016/S0005-2728(00)00286-3

28. Arai H, Kawakami T, Osamura T, Hirai T, Sakai Y, Ishii M. Enzymatic characterization and in vivo function of five terminal oxidases in Pseudomonas aeruginosa. J Bacteriol. 2014; 196: 4206–4215. https://doi.org/10.1128/JB.02176-14 PMID: 25182500

29. Rossi E, Falcone M, Molin S, Johansen HK. High-resolution in situ transcriptomics of Pseudomonas aeruginosa unveils genotype independent patho-phenotypes in cystic fibrosis lungs. Nat Commun. 2018; 9: 3459. https://doi.org/10.1038/s41467-018-05944-5 PMID: 30150613

30. Ray A, Williams HD. A mutant of Pseudomonas aeruginosa that lacks c-type cytochromes has a functional cyanide-insensitive oxidase. FEMS Microbiol Lett. 1996; 135: 123–129. https://doi.org/10.1111/j.1574-6968.1996.tb07976.x PMID: 8598268

31. Osamura T, Kawakami T, Kido R, Ishii M, Arai H. Specific expression and function of the A-type cytochrome c oxidase under starvation conditions in Pseudomonas aeruginosa. Roop RM, editor. PLoS One. 2017; 12: e0177957. https://doi.org/10.1371/journal.pone.0177957 PMID: 28542449

32. Cunningham L, Williams HD. Isolation and characterization of mutants defective in the cyanide-insensitive respiratory pathway of Pseudomonas aeruginosa. J Bacteriol. 1995; 177: 432–438. https://doi.org/10.1128/jb.177.2.432-438.1995 PMID: 7814333

33. Brooks T, Keevil CW. A simple artificial urine for the growth of urinary pathogens. Lett Appl Microbiol. 1997; 24: 203–206. https://doi.org/10.1046/j.1472-765x.1997.00378.x PMID: 9080700

34. Banin E, Brady KM, Greenberg EP. Chelator-Induced Dispersal and Killing of Pseudomonas aeruginosa Cells in a Biofilm. Appl Environ Microbiol. 2006; 72: 2064–2069. https://doi.org/10.1128/AEM.72.3.2064-2069.2006 PMID: 16517655

35. Schoenmakers TJ, Visser GJ, Flik G, Theuvenet AP. CHELATOR: an improved method for computing metal ion concentrations in physiological solutions. Biotechniques. 1992; 12: 870–4, 876–9. Available: http://www.ncbi.nlm.nih.gov/pubmed/1642895

36. Maiuolo J, Oppedisano F, Gratteri S, Muscoli C, Mollace V. Regulation of uric acid metabolism and excretion. Int J Cardiol. 2016; 213: 8–14. https://doi.org/10.1016/j.ijcard.2015.08.109 PMID: 26316329

37. Kahm M, Hasenbrink G, Lichtenberg-Fraté H, Ludwig J, Kschischo M. grofit: Fitting Biological Growth Curves with R. J Stat Softw. 2015; 33: 1–21. https://doi.org/10.18637/jss.v033.i07

38. Tuz K, Mezic KG, Xu T, Barquera B, Juárez O. The kinetic reaction mechanism of the vibrio cholerae sodium-dependent NADH dehydrogenase. J Biol Chem. 2015; 290: 20009–20021. https://doi.org/10.1074/jbc.M115.658773 PMID: 26004776

39. Wittig I, Braun HP, Schägger H. Blue native PAGE. Nat Protoc. 2006; 1: 418–428. https://doi.org/10.1038/nprot.2006.62 PMID: 17406264

40. Juárez O, Guerra G, Martínez F, Pardo JP. The mitochondrial respiratory chain of Ustilago maydis. Biochim Biophys Acta—Bioenerg. 2004; 1658: 244–251. https://doi.org/10.1016/j.bbabio.2004.06.005 PMID: 15450962

41. Barquera B, Häse CC, Gennis RB. Expression and mutagenesis of the NqrC subunit of the NQR respiratory Na + pump from Vibrio cholerae with covalently attached FMN. FEBS Lett. 2001; 492: 45–49. https://doi.org/10.1016/s0014-5793(01)02224-4 PMID: 11248234

42. Liang P, Rosas-Lemus M, Patel D, Fang X, Tuz K, Oscar Juárez X. Dynamic energy dependency of Chlamydia trachomatis on host cell metabolism during intracellular growth: Role of sodium-based energetics in chlamydial ATP generation. J Biol Chem. 2018; 293: 510–522. https://doi.org/10.1074/jbc.M117.797209 PMID: 29123027

43. Gong H, Li J, Xu A, Tang Y, Ji W, Gao R, et al. An electron transfer path connects subunits of a mycobacterial respiratory supercomplex. Science (80-). 2018; 362: eaat8923. https://doi.org/10.1126/science.aat8923 PMID: 30361386

44. Matsunaga K, Enjoji M, Karube Y, Takata J. Enhanced Intracellular Delivery and Improved Antitumor Efficacy of Menaquinone-4. Vitamin K2—Vital for Health and Wellbeing. InTech; 2017. p. https://doi.org/10.5772/63343

45. Furt F, Oostende C Van, Widhalm JR, Dale MA, Wertz J, Basset GJC. A bimodular oxidoreductase mediates the specific reduction of phylloquinone (vitamin K1) in chloroplasts. Plant J. 2010; 64: 38–46. https://doi.org/10.1111/j.1365-313X.2010.04305.x PMID: 20626653

46. Chu P-H, Huang T-Y, Williams J, Stafford DW. Purified vitamin K epoxide reductase alone is sufficient for conversion of vitamin K epoxide to vitamin K and vitamin K to vitamin KH2. Proc Natl Acad Sci U S A. 2006; 103: 19308–13. https://doi.org/10.1073/pnas.0609401103 PMID: 17164330

47. Giannakopoulos X, Evangelou A, Kalfakakou V, Grammeniatis E, Papandropoulos I, Charalambopoulos K. Human bladder urine oxygen content: implications for urinary tract diseases. Int Urol Nephrol. 1997; 29: 393–401. https://doi.org/10.1007/bf02551103 PMID: 9405994

48. Wilson ML, Gaido L. Laboratory Diagnosis of Urinary Tract Infections in Adult Patients. Clin Infect Dis. 2004; 38: 1150–1158. https://doi.org/10.1086/383029 PMID: 15095222

49. BARR JG, RITCHIE JWK, HENRY O, EL SHEIKH M, EL DEEB K. Microaerophilic/anaerobic bacteria as a cause of urinary tract infection in pregnancy. BJOG An Int J Obstet Gynaecol. 1985; 92: 506–510. https://doi.org/10.1111/j.1471-0528.1985.tb01356.x PMID: 3994933

50. Worth PHL. Recurrent urinary infection with microaerophilic and anaerobic bacteria. British Medical Journal. 1980. p. 1285. https://doi.org/10.1136/bmj.281.6250.1285-b PMID: 7427674

51. Xie H, Buschmann S, Langer JD, Ludwig B, Michel H. Biochemical and biophysical characterization of the two isoforms of cbb3-Type cytochrome c oxidase from Pseudomonas stutzeri. J Bacteriol. 2014; 196: 472–482. https://doi.org/10.1128/JB.01072-13 PMID: 24214947

52. Petersen LC. The effect of inhibitors on the oxygen kinetics of cytochrome c oxidase. BBA—Bioenerg. 1977; 460: 299–307. https://doi.org/10.1016/0005-2728(77)90216-X

53. Leavesley HB, Li L, Prabhakaran K, Borowitz JL, Isom GE. Interaction of Cyanide and Nitric Oxide with Cytochrome c Oxidase: Implications for Acute Cyanide Toxicity. Toxicol Sci. 2008; 101: 101–111. https://doi.org/10.1093/toxsci/kfm254 PMID: 17906319

54. Di Tomaso G, Fedi S, Carnevali M, Manegatti M, Taddei C, Zannoni D. The membrane-bound respiratory chain of Pseudomonas pseudoalcaligenes KF707 cells grown in the presence or absence of potassium tellurite. Microbiology. 2002; 148: 1699–1708. https://doi.org/10.1099/00221287-148-6-1699 PMID: 12055290

55. Weiss SA, Bushby RJ, Evans SD, Jeuken LJC. A study of cytochrome bo3 in a tethered bilayer lipid membrane. Biochim Biophys Acta—Bioenerg. 2010; 1797: 1917–1923. doi:https://doi.org/10.1016/j.bbabio.2010.01.012

56. Mogi T, Ano Y, Nakatsuka T, Toyama H, Muroi A, Miyoshi H, et al. Biochemical and Spectroscopic Properties of Cyanide-Insensitive Quinol Oxidase from Gluconobacter oxydans. J Biochem. 2009; 146: 263–271. https://doi.org/10.1093/jb/mvp067 PMID: 19416958

57. Friedrich T, Steinmüller K, Weiss H. The proton-pumping respiratory complex I of bacteria and mito-chondria and its homologue in chloroplasts. FEBS Lett. 1995; 367: 107–111. https://doi.org/10.1016/0014-5793(95)00548-n PMID: 7796904

58. Barquera B, Zhou W, Morgan JE, Gennis RB. Riboflavin is a component of the Na+-pumping NADH-quinone oxidoreductase from Vibrio cholerae. Proc Natl Acad Sci. 2002; 99: 10322–10324. https://doi.org/10.1073/pnas.162361299 PMID: 12122213

59. Blaza JN, Bridges HR, Aragão D, Dunn EA, Heikal A, Cook GM, et al. The mechanism of catalysis by type-II NADH:quinone oxidoreductases. Sci Rep. 2017; 7: 40165. https://doi.org/10.1038/srep40165 PMID: 28067272

60. Degli Esposti M. Inhibitors of NADH–ubiquinone reductase: an overview. Biochim Biophys Acta—Bioe-nerg. 1998; 1364: 222–235. https://doi.org/10.1016/S0005-2728(98)00029-2

61. Nakayama Y, Hayashi M, Yoshikawa K, Mochida K, UNEMOTO T. Inhibitor studies of a new antibiotic, korormicin, 2-n-heptyl-4-hydroxyquinoline N-oxide and Ag+ toward the Na+-translocating NADH-qui-none reductase from the marine Vibrio alginolyticus. Biol Pharm Bull. 1999; 22: 1064–1067. https://doi.org/10.1248/bpb.22.1064 PMID: 10549856

62. Tuz K, Li C, Fang X, Raba DA, Liang P, Minh DDL, et al. Identification of the catalytic ubiquinone-binding site of vibrio cholerae sodium-dependent NADH dehydrogenase A NOVEL UBIQUINONE-BINDING MOTIF. J Biol Chem. 2017; 292: 3039–3048. https://doi.org/10.1074/jbc.M116.770982 PMID: 28053088

63. Ernster L, Dallner G, Azzone GF, Felice Azzone G, Azzone GF. Differential Effects of Rotenone and Amytal on Mitochondrial Electron and Energy Transfer. J Biol Chem. 1963; 238: 1124–1131. Available: http://www.jbc.org/content/238/3/1124

64. Lümmen P. Complex I inhibitors as insecticides and acaricides. Biochim Biophys Acta—Bioenerg. 1998; 1364: 287–296. https://doi.org/10.1016/S0005-2728(98)00034-6

65. Orazi G, O'Toole GA. Pseudomonas aeruginosa alters Staphylococcus aureus sensitivity to vancomy-cin in a biofilm model of cystic fibrosis infection. MBio. 2017; 8: e00873–17. https://doi.org/10.1128/mBio.00873-17 PMID: 28720732

66. Hazan R, Que YA, Maura D, Strobel B, Majcherczyk PA, Hopper LR, et al. Auto Poisoning of the Respi-ratory Chain by a Quorum-Sensing-Regulated Molecule Favors Biofilm Formation and Antibiotic Toler-ance. Curr Biol. 2016; 26: 195–206. https://doi.org/10.1016/j.cub.2015.11.056 PMID: 26776731

67. Kang J-W, Kim Y-J. HQNO-sensitive NADH:Quinone Oxidoreductase of Bacillus cereus KCTC 3674. BMB Rep. 2007; 40: 53–57. https://doi.org/10.5483/bmbrep.2007.40.1.053 PMID: 17244482

68. Fadeeva MS, Núñez C, Bertsova Y V., Espín G, Bogachev A V. Catalytic properties of Na+-translocat-ing NADH:quinone oxidoreductases from Vibrio harveyi, Klebsiella pneumoniae, and Azotobacter vine-landii. FEMS Microbiol Lett. 2008; 279: 116–123. https://doi.org/10.1111/j.1574-6968.2007.01015.x PMID: 18300384

69. Zhou W, Bertsova Y V., Feng B, Tsatsos P, Verkhovskaya ML, Gennis RB, et al. Sequencing and pre-liminary characterization of the Na+-translocating NADH:ubiquinone oxidoreductase from Vibrio har-veyi. Biochemistry. 1999; 38: 16246–16252. https://doi.org/10.1021/bi991664s PMID: 10587447

70. Liu J, Krulwich TA, Hicks DB. Purification of two putative type II NADH dehydrogenases with different substrate specificities from alkaliphilic Bacillus pseudofirmus OF4. Biochim Biophys Acta—Bioenerg. 2008; 1777: 453–461. https://doi.org/10.1016/j.bbabio.2008.02.004 PMID: 18359284

71. Björklöf K, Zickermann V, Finel M. Purification of the 45 kDa, membrane bound NADH dehydrogenase of Escherichia coli (NDH-2) and analysis of its interaction with ubiquinone analogues. FEBS Lett. 2000; 467: 105–110. https://doi.org/10.1016/s0014-5793(00)01130-3 PMID: 10664466

72. Berger A, Dohnt K, Tielen P, Jahn D, Becker J, Wittmann C. Robustness and plasticity of metabolic pathway flux among uropathogenic isolates of Pseudomonas aeruginosa. PLoS One. 2014; 9: e88368. https://doi.org/10.1371/journal.pone.0088368 PMID: 24709961

73. Kretzschmar U, Ru A, Jeoung J. Malate:quinone oxidoreductase is essential for growth on ethanol or acetate in Pseudomonas aeruginosa. Microbiology. 2002; 148: 3839–3847. https://doi.org/10.1099/00221287-148-12-3839 PMID: 12480887

74. Kemp MB. D- and L-Lactate Dehydrogenases of Pseudomonas aeruginosa. Biochem J. 1972; 130: 307–309. https://doi.org/10.1042/bj1300307 PMID: 4347789

75. Scheijen JLJM, Hanssen NMJ, Van De Waarenburg MPH, Jonkers DMAE, Stehouwer CDA, Schalkwijk CG. L(+) and D(-) lactate are increased in plasma and urine samples of type 2 diabetes as measured by a simultaneous quantification of L(+) and D(-) lactate by reversed-phase liquid chromatography tandem mass spectrometry. Exp Diabetes Res. 2012; 2012: 1–10. https://doi.org/10.1155/2012/234812 PMID: 22474418

76. Kawakami T, Kuroki M, Ishii M, Igarashi Y, Arai H. Differential expression of multiple terminal oxidases for aerobic respiration in *Pseudomonas aeruginosa*. Environ Microbiol. 2009; 12: 1399–412. https://doi.org/10.1111/j.1462-2920.2009.02109.x PMID: 19930444

77. Ugidos A, Morales G, Rial E, Williams HD, Rojo F. The coordinate regulation of multiple terminal oxidases by the Pseudomonas putida ANR global regulator. Environ Microbiol. 2008; 10: 1690–1702. https://doi.org/10.1111/j.1462-2920.2008.01586.x PMID: 18341582

78. Tseng CP, Albrecht J, Gunsalus RP. Effect of microaerophilic cell growth conditions on expression of the aerobic (cyoABCDE and cydAB) and anaerobic (narGHJI, frdABCD, and dmsABC) respiratory pathway genes in Escherichia coli. J Bacteriol. 1996; 178: 1094–1098. https://doi.org/10.1128/jb.178.4.1094-1098.1996 PMID: 8576043

79. Richhardt J, Luchterhand B, Bringer S, Büchs J, Bott M. Evidence for a key role of cytochrome bo3 oxidase in respiratory energy metabolism of Gluconobacter oxydans. J Bacteriol. 2013; 195: 4210–20. https://doi.org/10.1128/JB.00470-13 PMID: 23852873

80. Comolli JC, Donohue TJ. Differences in two Pseudomonas aeruginosa cbb3 cytochrome oxidases. Mol Microbiol. 2004; 51: 1193–1203. https://doi.org/10.1046/j.1365-2958.2003.03904.x PMID: 14763990

81. Jo J, Cortez KL, Cornell WC, Price-Whelan A, Dietrich LEP. An orphan cbb3-type cytochrome oxidase subunit supports Pseudomonas aeruginosa biofilm growth and virulence. Elife. 2017;6. https://doi.org/10.7554/eLife.30205 PMID: 29160206

82. Zlosnik JEA, Tavankar GR, Bundy JG, Mossialos D, O'Toole R, Williams HD. Investigation of the physiological relationship between the cyanide-insensitive oxidase and cyanide production in Pseudomonas aeruginosa. Microbiology. 2006; 152: 1407–1415. https://doi.org/10.1099/mic.0.28396-0 PMID: 16622057

83. Puustinen A, Finel M, Haltia T, Gennis RB, Wikström M. Properties of the two terminal oxidases of Escherichia coli. Biochemistry. 1991; 30: 3936–42. Available: http://www.ncbi.nlm.nih.gov/pubmed/1850294 doi: 10.1021/bi00230a019 PMID: 1850294

84. Borisov VB, Gennis RB, Hemp J, Verkhovsky MI. The cytochrome bd respiratory oxygen reductases. Biochim Biophys Acta—Bioenerg. 2011; 1807: 1398–1413. https://doi.org/10.1016/j.bbabio.2011.06.016 PMID: 21756872

85. Hoboth C, Hoffmann R, Eichner A, Henke C, Schmoldt S, Imhof A, et al. Dynamics of Adaptive Microevolution of Hypermutable Pseudomonas aeruginosa during Chronic Pulmonary Infection in Patients with Cystic Fibrosis. J Infect Dis. 2009; 200: 118–130. https://doi.org/10.1086/599360 PMID: 19459782

86. Merrell DS, Hava DL, Camilli A. Identification of novel factors involved in colonization and acid tolerance of Vibrio cholerae. Mol Microbiol. 2002; 43: 1471–1491. https://doi.org/10.1046/j.1365-2958.2002.02857.x PMID: 11952899

87. Petri J, Shimaki Y, Jiao W, Bridges HR, Russell ER, Parker EJ, et al. Structure of the NDH-2 –HQNO inhibited complex provides molecular insight into quinone-binding site inhibitors. Biochim Biophys Acta—Bioenerg. 2018; 1859: 482–490. https://doi.org/10.1016/j.bbabio.2018.03.014 PMID: 29621505

88. Liberati NT, Urbach JM, Miyata S, Lee DG, Drenkard E, Wu G, et al. An ordered, nonredundant library of Pseudomonas aeruginosa strain PA14 transposon insertion mutants. Proc Natl Acad Sci U S A. 2006; 103: 2833–2838. https://doi.org/10.1073/pnas.0511100103 PMID: 16477005

89. Deziel E, Lepine F, Milot S, He J, Mindrinos MN, Tompkins RG, et al. Analysis of Pseudomonas aeruginosa 4-hydroxy-2-alkylquinolines (HAQs) reveals a role for 4-hydroxy-2-heptylquinoline in cell-to-cell communication. Proc Natl Acad Sci. 2004; 101: 1339–1344. https://doi.org/10.1073/pnas.0307694100 PMID: 14739337

90. Dietrich LEP, Okegbe C, Price-Whelan A, Sakhtah H, Hunter RC, Newmana DK. Bacterial community morphogenesis is intimately linked to the intracellular redox state. J Bacteriol. 2013; 195: 1371–1380. https://doi.org/10.1128/JB.02273-12 PMID: 23292774

91. Reyes-Prieto A, Barquera B, Juárez O. Origin and evolution of the sodium -pumping NADH: Ubiquinone oxidoreductase. PLoS One. 2014; 9: 1–14. https://doi.org/10.1371/journal.pone.0096696 PMID: 24809444

92. Bogachev A V., Kulik L V., Bloch DA, Bertsova Y V., Fadeeva MS, Verkhovsky MI. Redox properties of the prosthetic groups of Na + -translocating NADH:quinone oxidoreductase. 1. Electron paramagnetic resonance study of the enzyme. Biochemistry. 2009; 48: 6291–6298. https://doi.org/10.1021/bi900524m PMID: 19496621

93. Steuber J, Vohl G, Muras V, Toulouse C, Claußen B, Vorburger T, et al. The structure of Na$^+$-translocating of NADH:Ubiquinone oxidoreductase of Vibrio cholerae: Implications on coupling between electron transfer and Na$^+$ transport. Biol Chem. 2015; 396: 1015–1030. https://doi.org/10.1515/hsz-2015-0128 PMID: 26146127

94. Van Ark G, Berden JA. Binding of HQNO to beef-heart sub-mitochondrial particles. BBA—Bioenerg. 1977; 459: 119–137. https://doi.org/10.1016/0005-2728(77)90014-7

95. Matsushita K, Patel L, Kaback HR. Cytochrome o Type Oxidase from Escherichia coli. Characterization of the Enzyme and Mechanism of Electrochemical Proton Gradient Generation. Biochemistry. 1984; 23: 4703–4714. https://doi.org/10.1021/bi00315a028 PMID: 6093862

96. Bogachev A V., Murtasina RA, Shestopalov AI, Skulachev VP. The role of protonic and sodium potentials in the motility of E. coli and Bacillus FTU. BBA—Bioenerg. 1993; 1142: 321–326. https://doi.org/10.1016/0005-2728(93)90160-H

97. STANNARD JN, HORECKER BL. The in vitro inhibition of cytochrome oxidase by azide and cyanide. J Biol Chem. 1948; 172: 599–608. PMID: 18901179